We are IntechOpen, the world's leading publisher of Open Access books Built by scientists, for scientists

4,800
Open access books available

122,000
International authors and editors

135M
Downloads

Our authors are among the

154
Countries delivered to

TOP 1%
most cited scientists

12.2%
Contributors from top 500 universities

CLARIVATE ANALYTICS BOOK CITATION INDEX INDEXED

WEB OF SCIENCE™

Selection of our books indexed in the Book Citation Index in Web of Science™ Core Collection (BKCI)

Interested in publishing with us?
Contact book.department@intechopen.com

Numbers displayed above are based on latest data collected.
For more information visit www.intechopen.com

Chapter 5

Noble Metal Nanoparticles Prepared by Metal Sputtering into Glycerol and their Grafting to Polymer Surface

Jakub Siegel, Alena Řezníčková, Petr Slepička and Václav Švorčík

Additional information is available at the end of the chapter

http://dx.doi.org/10.5772/61403

Abstract

This chapter summarizes the basic information about elementary characteristics and technology of preparation of noble metal nanoparticles. The introduction gives some basic information on the history of development in this area, especially in terms of dimensionality of metal nanostructures and their possible applications.The first subsection is devoted to the preparation and characterization of Au, Ag, Pt, and Pd nanoparticles (NPs), which were synthesized by direct metal sputtering in liquid propane-1,2,3,-triole (glycerol). This method provides an interesting alternative to time-consuming, wet-based chemical synthesis techniques. Moreover, the suggested technique allows targeted variation of metal nanoparticle size, which is demonstrated in detail in case of AuNPs by variation of capturing media temperature. Nanoparticle size and shape were studied by transmission electron microscopy and dynamic light scattering. Optical properties of nanoparticle solution were determined by measuring its UV–Vis spectra. Concentration of metal nanoparticles in prepared solutions was determined by atomic absorption spectroscopy. Antibacterial properties were tested against two common pollutants (*Escherichia coli*, a Gram-negative bacteria, and *Staphylococcus epidermidis*, a Gram-positive bacteria). In the presence of Ag nanoparticles, the growth of *E. coli* and *S. epidermidis* was completely inhibited after 24 h. Any growth inhibition of *E. coli* was observed neither in the presence of "smaller" (4–6 nm, $AuNP_{4–6}$) nor "bigger" (9–12 nm, $AuNP_{8–12}$) AuNPs during the whole examination period. $AuNP_{4–6}$, but not $AuNP_{8–12}$, was able to inhibit the growth of. *S epidermidis*. We also observed significant difference in biological activities of Pt and PdNPs. More specifically, PdNPs exhibited considerable inhibitory potential against both *E. coli* and *S. epidermidis*, which was in contrast to ineffective PtNPs. Our results indicate that Ag, Pd, and partially AuNPs have high potential to combat both Gram-positive and Gram-negative bacterial strains.The second subsection describes the effort to anchor metal nanoparticles onto polyethyleneterephthalate (PET) carrier. Two different procedures of grafting of polymeric carrier, activated by plasma treatment, with Au and AgNPs are described. In the first procedure, the PET foil was grafted with biphenyl-4,4′-dithiol (BPD) and subsequently with Au and AgNPs. In the second one, the PET foil was grafted with Au and AgNPs previously coated by the same BPD. X-ray photoelectron spectrosco-

py, Fourier transform infrared spectroscopy, and electrokinetic analysis were used for characterization of the polymer surface at different modification steps. Au and AgNPs were characterized by UV–Vis spectroscopy. In case of both types of nanoparticles, the first procedure was found to be more effective. It was proved that the BPD was chemically bonded to the surface of the plasma-activated PET and it mediates subsequent grafting of the AuNPs.

Keywords: Nanoparticles, sputtering, antibacterial effect, chemical anchoring, polymer

1. Introduction

Metal nanoparticles (NPs) nowadays represent the key material in vast range of industrial applications ranging from rough industry to fine medical or biochemical utilization. Gold and silver NPs and their applications are currently of great interest. In recent years, rapid developments in nanotechnology have evolved to the point where inclusion of those entities into smart systems and related technologies has become quite easy. Nowadays, NPs and NPs-embedded materials cover broad spectrum of functional devices with promising properties, which are used in many fields including optoelectronics or catalysis [1]. They are employed in modern nanobiotechnology for the production of biosensors, visualization of cellular structures [2], and targeted transporting of drugs [3]. Colloidal nanoparticles are studied because they have unique physical and chemical properties that are different from "bulk" materials [4]. In all applications of nanotechnology, the size and shape of the nanoparticles play an important role [5]. Numerous studies [6] describe the unique properties of gold nanoparticles which can be used in applications such as fuel cells, environmental, and other chemical processes [7]. Various preparation techniques have been proposed to cover specific requirements of those man-made entities. Besides classical wet-based preparation techniques of which the pioneering one is that proposed by Turkevich [8], others are intensely studied which would open up new potential applications of NPs in the development of new technologies.

NPs are entities ranging in size between 1 to 100 nanometres. These materials behave as a whole unit in terms of transportation and properties that highly depend on their shape, size, and morphological substructure [9, 10]. Those materials are characterized by high surface area-to-volume ratio, high chemical reactivity and physical affinity, as well as other interesting physico-chemical properties (optical, electrical, and magnetic) [11–14]. In addition, different NPs show various properties; likewise, different synthesis techniques of the same type of particle tend to alter or introduce new properties to the material. Consequently, the applications of these materials are unlimited and significantly remarkable in human life and in industries. Each nanomaterial with its distinct properties independently finds its way into practical applications such as: drug delivery [15], waste treatment [16], lubricant and surfactant production [17], electrical and sensor devices [18, 19], as well as membrane fuel cells [20]. Noble metal NPs have been widely studied in the past few decades because of their applications in

http://dx.doi.org/10.5772/61403

various areas including catalysis, gas and biological sensors, drug delivery, and antimicrobial agents. In specific, due to their biocompatibility and photo-optical distinctiveness, gold NPs (AuNPs) have proven to be very useful tools in several biomedical applications dealing with different aspects of detection, analysis, and treatment.

Recent advances in the study of noble metal NPs have led to their utilization in a number of very important applications including antimicrobial coatings, biosensing, diagnostic imaging, and cancer diagnosis and therapy [21–24]. This chapter surveys the various synthetic methods of broad spectrum of metallic NPs as well as most recent experimental studies focusing on the use of gold, silver, palladium, platinum, and ruthenium NPs in catalysis, food industry, and environmental applications. Moreover, the potent in vitro and in vivo antimicrobial and cytogenotoxic effects of various gold and silver nanomaterials are underlined. Finally, recent advances in functionalization of various solid substrates with gold and silver NPs as effective antimicrobial coatings and promising cell-stimulating agents are summarized. Despite their use in remediating numerous medical and health-related conditions, the efficacy and safety of many gold, silver, palladium, and platinum NPs are still under some scrutiny.

2. Nanoparticle synthesis

One of the most common nanoparticle synthesis of noble metals are those developed by Brust–Schiffrin [25]. The technique is based on reduction of Au^{III+} complex compound with $NaBH_4$ stabilized by thiols. This technique enables preparation of highly stable particles with narrow distribution and possibility to control their sizes. Also, Ag particles have already been synthesized on the basis of reduction reactions [7,8]. Concurrently, due to specific requirements on newly synthesized NPs, there have arisen other numerous techniques based on both wet and dry processes. Nowadays, most of the wet-based preparation techniques exploit confined reaction area inside which metal ions are reduced to zerovalent metals forming nanoparticles. The smaller and uniform the reaction cavity is, the smaller the dimension and narrower the size distribution of the resulting NPs. Different types of polymer-based agents have been investigated for preparation of metal and non-metal particles [26–31]. Metal NPs, semiconductors, inorganic oxides, and quantum dots synthesis were also investigated, especially in the confined space of surfactants, inorganic templates, and polymeric stabilizing agents [32–35]. The structure of the metal particles can be significantly affected by the preparation technique [36–39]. Their size, shape, and geometry strongly depend on the applied technique. Therefore, it is very important to use a template that is modifiable in terms of functional groups and is adjustable with respect to its shape or size. Polymeric hydrogels are able to fulfil these parameters, and they can be also successfully prepared in various sizes with different functional groups [26, 40].

Butun and Sahiner [41] reported synthesis of a novel bulk hydrogel based on acrylamidoglycolic acid and its use as a template in the preparation of different metal NPs (Ag, Cu, Ni, Co). Nanoparticle synthesis is based on reduction of the captured metal ions inside the hydrogel.

Hydrogels play a key role in tissue engineering because of the resemblance of the three-dimensional network structure to the extracellular matrix environment [42–44]. The bulk hydrogels consist mostly of macropores (>50 nm) and even superpores with the pore sizes of up to several microns. The porosity can be modified by the degree of functional groups hydrophilicity or by the cross-linker used during preparation. The tune capability of the pore structure also provides specific advantages for the absorption and desorption of various species [45].

Completely new possibilities for the preparation of metal NPs open up utilization of PVD techniques. The most common capturing media for direct metal sputtering represent ion liquids (ILs) and their significantly less-toxic alternative – vegetable oils. First metal deposition onto liquid substrate was conducted in 1996 by the mean of radiofrequency (RF) magnetron sputtering. Silver was deposited into pure silicon oil [46]. The process went through two stages: (i) creation of percolation structure and (ii) nucleation of first metal clusters on the oil surface. With ongoing deposition, individual clusters spread out over the liquid surface and mutually interconnected forming continuous silver coverage floating on the oil surface. Such Ag layer exhibited considerable roughness with typical morphology. Sputtering process was strongly dependent on deposition conditions; when the sputtering power was held below 30 W, no silver layer was formed. Most probably, the drop of the sputtering power resulted in penetration of silver atoms into the liquid volume and formation of silver NPs (AgNPs). Nevertheless, this finding was not confirmed by the authors since their intention was to prepare ultra-thin silver layers on the surface of liquid [47].

Vegetable oils represent perspective liquid substrates for sputtering of metals, since they are commonly available, cheap, biocompatible, and have the ability to stabilize metal NPs [48] (e.g., by the way of chemical reduction [49]). Thus, for the successful preparation of nanoparticles, no other toxic reducing agents are required, which is very desirable for further in vivo applications. Direct sputtering of Au into castor oil results in formation of biocompatible AuNPs. Application of higher voltage led to creation of larger particles, while the prolongation of deposition time had no impact on nanoparticle size, which was proved by transmission electron microscopy (TEM) and small angle Y-ray scattering (SAXS) [48]. Wender et al. [50] published interesting work correlating the properties of specific oil used with the deposition conditions with regards to formation of thin layers on the surface or in the volume of the oil. Authors showed that formation of AgNPs depends crucially on the applied voltage and specific surface coordination ability of the oil used (castor, canola, and kapron oil). Both lower voltage and weak coordination ability led to formation of continuous coatings on the oil surface. On contrary, higher voltage and strong coordination ability enable preparation of NPs. Higher voltage means higher diffusivity of adsorbed particles (metal atoms) on the surface of liquid which enables (i) particle penetration into the volume of liquid and (ii) anchoring of atoms/clusters to active functional groups. AgNPs were easily formed in castor oil (which contains solely hydroxyl groups) in wide range of applied voltage. On contrary, when using canola oil (which is predominately formed by unsaturated aliphatic chains) and kapron oil,

http://dx.doi.org/10.5772/61403

thin silver layer was deposited on the oil surface at lower voltages, while AgNPs were formed only at higher discharge voltage.

Much more aggressive media (from the toxicity point of view) for potential biomedical application of prepared NPs are already mentioned ILs. Those liquids can be defined as liquid electrolytes exclusively composed of ions. Currently, the most common ILs are pure substances or eutectic mixtures of organic–inorganic salts, which melts at temperatures below 100°C [51]. Among the most widespread ILs belong derivates of organic molecules, e.g., pyrrolidine, imidazole, and pyridine [52]. ILs' attractiveness in the process of NPs preparation consists in unusual physical–chemical properties. In addition to their extreme polarity, they also exhibit very low value of interface tension. Considering this, relatively high speed of nucleation can be achieved during the deposition process, which results in formation of small NPs without undesirable perturbations (Ostwald ripening[1]) [53]. Moreover, ILs very easily change their molecular arrangement so that to adapt to nucleation centres of emerging NPs, which leads to their stabilization. This high degree of adaptability consists in the presence of both hydrophilic and hydrophobic segments together with strong polarization force of ILs, which enables their orientation both perpendicular and parallel to the particles [13].

A large number of authors regard the value of surface tension and viscosity of liquid as critical in the process of preparation of metal NPs in liquid media. However, as evidenced in the work [52], in particular in the case of ILs, other parameters such as composition and the coordinating ability of the used liquid also play a significant role. If in addition the NPs growth occurs in the liquid volume, increase in the NPs size with increasing volume (size) of ILs anionic part can be expected [54–57]. Furthermore, it appears that the difference in size of the synthesized particles cannot be correlated with macroscopic characteristics of ILs, such as surface tension and viscosity [54]. In this connection, a very interesting medium for preparation of NPs by metal sputtering into liquid is pure propane-1,2,3-triole (glycerol) [31]. This substance combines physical properties comparable to those of ILs (i.e., low vapor pressure, thermally manageable viscosity, high coordination ability – per one glycerol molecule falls three hydroxyl groups) with minimal toxicity to living tissues. Biocompatibility of glycerol allows subsequent application of prepared NPs in bioengineering [58]. Additionally, one can easily control the size of emerging particles by the temperature of the capturing media (glycerol). Recent advances in preparation ways of selected noble metal NPs are summarized in Table 1.

Besides all other noble metals, silver in the form of AgNPs possesses strong antimicrobial specificity. The AgNPs use is of great importance, since several pathogenic bacteria have developed resistance to different types of antibiotics. That is why AgNPs have emerged up with varied medical applications reaching from silver-based dressings, silver-coated medicinal devices (nanogels, nanolotions), etc. The antibacterial effects of Ag salts have been noticed since antiquity [59], and Ag is currently used to control bacterial growth in a wide spectrum of applications, including dental work, catheters, and burn wounds [60, 61]. In fact, it is well

1 Mass transfer from smaller particles to larger particles extending in real polydisperse systems as a result of higher vapour pressure or greater solubility of smaller particles. This reduction of the degree of dispersion proceeds until the conversion of disperse systems into the system with sufficiently coarse dispersion in which the differences in solubility or vapour pressure of particles of different sizes are a very slight, and the process speed is negligibly small.

known that Ag ions and Ag-based compounds are highly toxic to microorganisms, showing strong biocidal effects on as many as more than ten species of bacteria including *E. coli* [62, 63].

Type of NPs					Synthetic method	NP size	References
Au	Ag	Pd	Pt	Cu		(nm)	
•					Sol–gel microreactors	5–50	[64, 65]
•	•	•	•		PVD into liquid substrate	2–5	[21, 31]
		•	•		Reduction in acidic environment	3–40	[66]
•					Reduction process	2–40	[25, 67–70]
•				•	γ-Irradiation	3–30	[71]
				•	pH control of Cu complexes	48–150	[72]
•	•	•			Biosynthesis	9–25	[73–77]
	•				Wet chemistry	20–60	[78, 79]

Table 1. Preparation techniques of selected noble metals with their typical size distributions.

Particle size reduction is an efficient and dependable tool to improve their bactericidal action and cytocompatibility. Nanotechnology techniques are of great assistance in the process of overcoming the limitations of size of nanoparticles [80]. Nanomaterials can be modified with the aim of better efficiency to facilitate their applications in various fields, e.g., bioscience and medicine.

3. Gold, silver, platinum, and palladium nanoparticles physically deposited into glycerol

In this section, a brief overview on results published by our group in the field of noble metal nanoparticles synthesis and investigation of their antibacterial action is introduced. The antimicrobial effects of Au, Ag, Pt, and PdNPs were tested against representative microorganisms of public concern. When applying metal NPs into living tissues, fundamental attention must be paid to their synthesis process itself. For successive, non-invasive application of metal NPs into living microorganisms, our group has developed a novel, unconventional approach for the physical synthesis of gold, silver, platinum, and palladium NPs based on direct metal sputtering into the liquid media (glycerol) [21, 31]. Considering this, direct metal deposition into the glycerol seems to be a promising technique combining the advantages of non-toxic and environmentally friendly process completely omitting the usage of solvents or reduction agents compared to classical wet-based methods. Furthermore, the possibility of tailoring the NP size via controlling the temperature of capturing media as well as the investigation of the functions of NP size and metal type (gold and silver) on the antibacterial activity are demonstrated. The antibacterial properties of these NPs were tested against two

http://dx.doi.org/10.5772/61403

common pollutants of *Escherichia coli* (*E. coli*, Gram-negative bacteria) and *Staphylococcus epidermidis* (*S. epidermidis*, Gram-positive bacteria) naturally occurring on the skin and mucous membranes of human and frequently involved in infections associated with a biofilm formation. Prepared NPs were characterized by transmission electron microscopy with or without high-resolution (HRTEM, TEM) and UV–Vis spectroscopy.

TEM images of Au and Ag NPs are shown in Figure 1 [31]. Both Au and Ag NPs possess spherical shape with average diameter of about 3.5 and 2.4 nm, respectively. It was shown that the NPs size distribution and uniformity remain untouched even in diluted aqueous solutions up to glycerol:water ratio of 1:20. It is a well-known fact that the presence of glycerol –OH group stabilizes aqueous solution of AgNPs [81]. But the stabilization role of glycerol –OH groups in AuNPs is not yet fully understood. Inset in Figure 1A introduces TEM image of AuNPs, which were stored 3 months at ambient conditions. The agglomeration of particles can be seen, which is in accordance with UV–Vis analysis. Contrary to that, this phenomenon was not found in case of AgNPs.

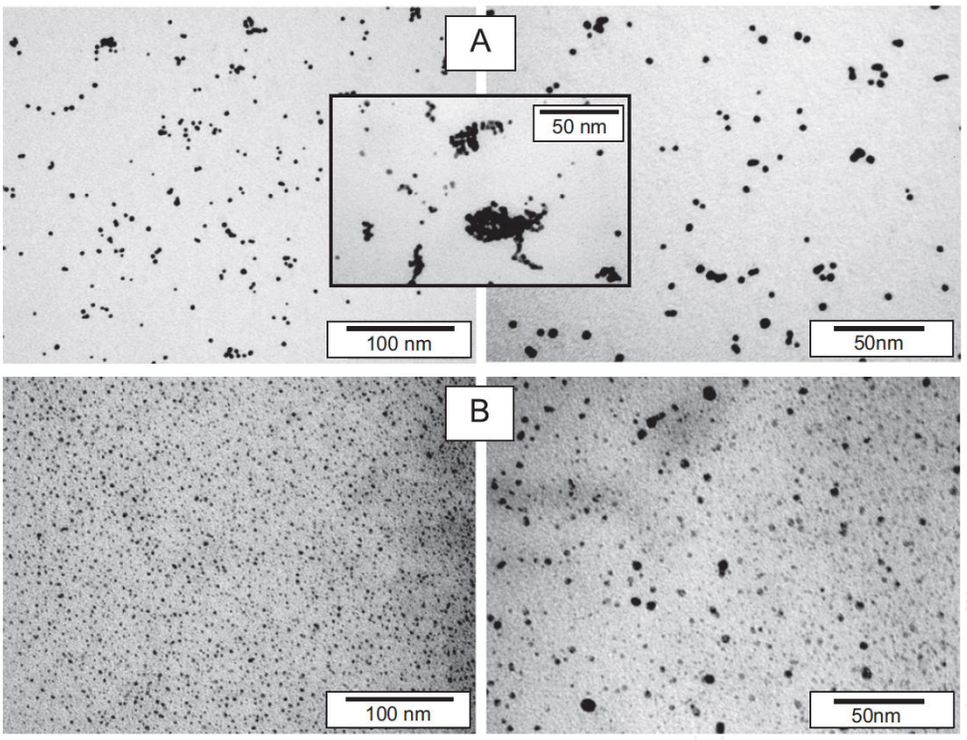

Figure 1. TEM images of Au (A) and Ag (B) nanoparticles. Inset in (A) shows TEM image of Au nanoparticles after 3 months storage at laboratory conditions [31].

UV–Vis absorption spectra measured on Au and AgNPs solutions promptly after deposition (solid lines) and after 3 month storage at ambient conditions (dash lines) are introduced in Figure 2 and discussed in detail in [31]. UV–Vis is often used to estimate size, shape, and particle size distribution of colloidal solutions of metal nanoparticles as they show specific absorption band corresponding to localized surface plasmon resonance (LSPR) [82, 83]. Nevertheless, this method must be conducted under precise and reproducible conditions, since the position and

intensity of LSPR absorption peak are affected by many factors, e.g., used solvents, type of stabilizers, and counter ions. The shape of the spectra exhibiting significant LSPR peaks corresponds to uniform nanoparticle colloidal solutions and also corresponds to the narrow size distribution [12, 84]. UV–Vis absorption spectrum of Au sample measured directly after deposition (solid line) shows diminishing LSPR peak with maximum at 512 nm. The shape and position of this peak suggest the particle sizes to be in interval from 2 to 10 nm [82], which corresponds with the sample's type (aqueous solution). Nevertheless, the influence of the AuNPs stabilization by –OH groups on the peak shift is not yet fully known. Mild red shift in spectrum after 3 month storage indicates both agglomeration effect and less narrow distribution compared to original sample. Narrow and high-intensity peak occurring at 400 nm together with the pure yellow coloration of the colloid solution indicates the presence of zerovalent Ag. Oxidized AgNPs do not exhibit this peak in their UV–Vis spectrum [85]. Contrary to AuNPs, AgNPs solution is much more stable even after 3 months storage. The corresponding spectrum exhibits almost the same peak position with pretty narrow distribution.

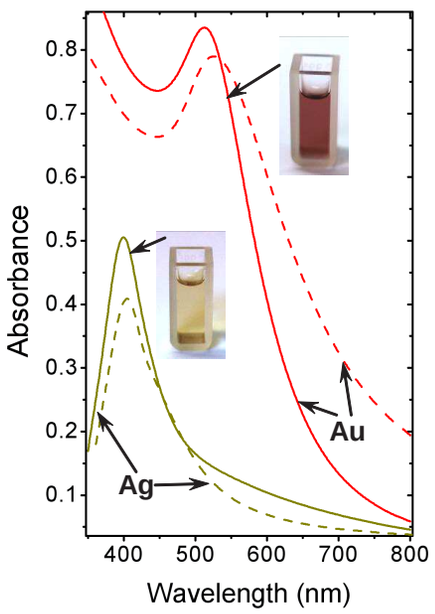

Figure 2. UV–Vis absorption spectra of Au and Ag aqueous nanoparticle solutions together with the photographs of corresponding NP solutions. Dash lines represent UV–Vis spectra of Au and Ag aqueous nanoparticle solutions stored for 3 months at laboratory conditions [31].

Targeted variation of metal nanoparticle size belongs to the great challenges of current science. Variation of capturing media temperature may provide a broad spectrum of nanoparticle diameters. The control of nanoparticle size through the capturing media temperature may be expressed upon a simple, generally known approach [86], which states that nanoparticle growth is governed by diffusion from the bulk of colloidal dispersion to the solution/particle interphase. When applied this approach, both $AgNP_{4–6}$ and $AuNP_{4–6}$ (indexes refer to average nanoparticle size) exhibit distinctive narrow peaks with maximum absorption at 400 and 520 nm, respectively (see Figure 3) [58]. These spectra are almost identical to those obtained in our former study on Ag and Au with average diameter of 3–5 nm, indicating stable solutions with

http://dx.doi.org/10.5772/61403

minimal particle dispersion. Considerable broadening with pronounced red shift of absorption peek occurs at $AuNP_{9–12}$. This phenomenon originates from both, increase in dimensions of individual Au particles and broader size distribution compared to $AuNP_{4–6}$. Distinctive red coloration of $AuNP_{4–6}$ turns into purple one, belonging to $AuNP_{9–12}$, as the average size increases from ca 5 to 10 nm (see Figure 4).

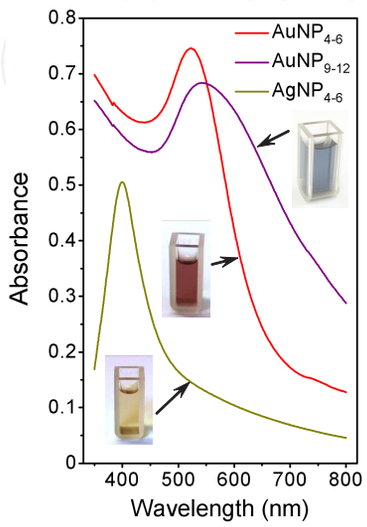

Figure 3. UV–Vis absorption spectra of Ag ($AgNP_{4–6}$) and Au ($AuNP_{4–6}$, $AuNP_{9–12}$) aqueous solutions of different nanoparticle size together with the photographs of corresponding NP solutions (indexes refer to average NP diameter in nm) [58].

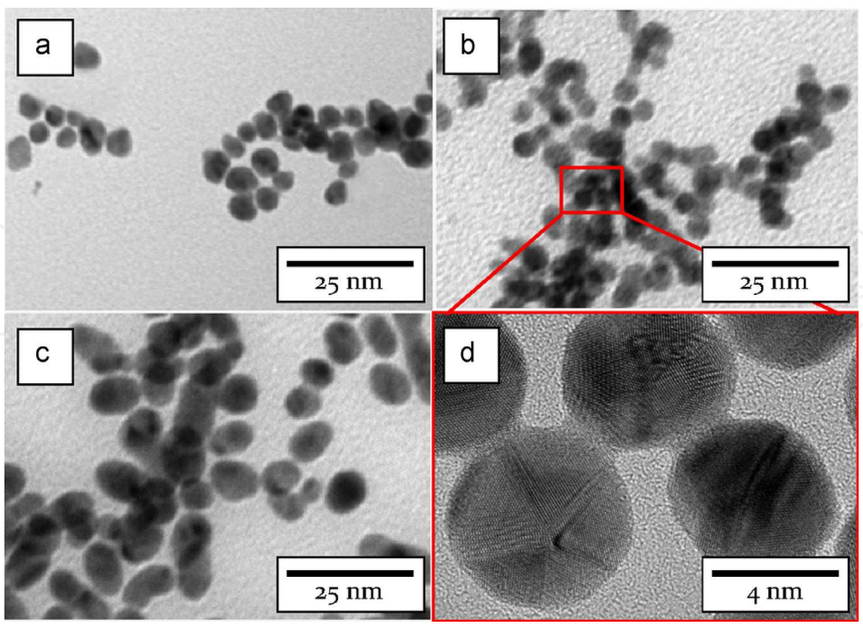

Figure 4. TEM images of nanoparticles of different composition and size $AgNP_{4–6}$ (a), $AuNP_{4–6}$ (b), and $AuNP_{9–12}$ (c), together with detailed HRTEM image of corresponding area (d). Indexes refer to NP diameter in nm [58].

Generally, two major aspects determine whether the growth of NPs during metal sputtering into liquids will take a place rather than formation of thin film on the liquid surface [52]. Firstly, the kinetic energy of sputtered atoms or clusters must be sufficient to penetrate the surface of capturing media. Secondly, the first condition may be fulfilled only in the limited range of media viscosity; thus, the liquid media cannot be too viscous. When those conditions are met, the formation of NPs occurs. Figure 5 shows TEM and HRTEM images of diluted aqueous solutions of Pt and PdNPs. Image analysis of more than 500 particles from 10 different areas of TEM pictures proved that prepared PtNPs and PdNPs have average diameter of (1.7 ± 0.3) nm and (2.4 ± 0.4) nm, respectively. Apparent aggregation of particles is due to the preparation method of samples for TEM (HRTEM) analysis. Observed discrepancy in particle size is probably due to different sputtering yield of both metals (Pt ~ 1.27, Pd ~ 2.09) [87], which is in accordance with supposed growth mechanism causes considerably slower growth of Pt particles (lower concentration gradient).

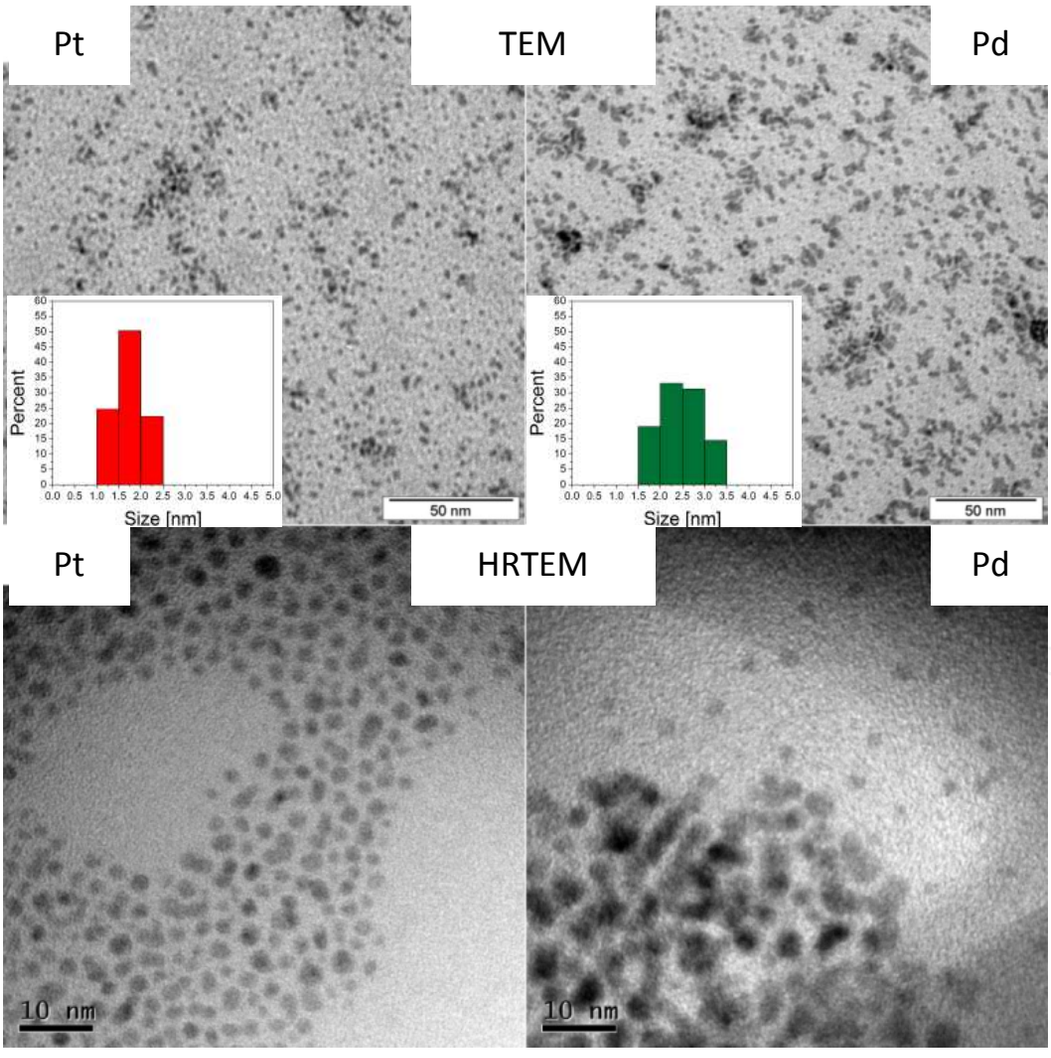

Figure 5. TEM and HRTEM images of diluted aqueous solutions of Pt and PdNPs insets show histogram of corresponding particle size and distribution [21].

http://dx.doi.org/10.5772/61403

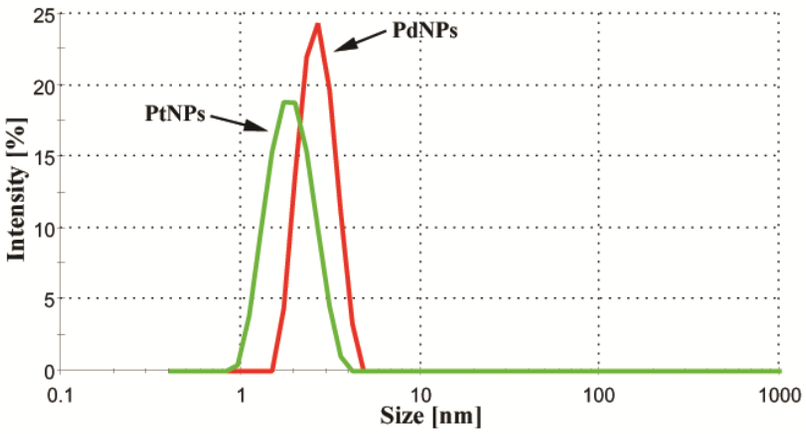

Figure 6. Characterization of aqueous solutions with metal nanoparticles by dynamic light scattering. Green line refers to PtNPs and red one PdNPs [21].

Additionally to TEM analysis, DLS measurement was accomplished to determine average size and size distribution of prepared NPs (see Figure 6, previous page). DLS measurements indicates that both particles are about 7% bigger compared to TEM-based analysis, which is in a good agreement with the published results [88], since DLS technique provides hydrodynamic diameter. Moreover, observed size discrepancy is inherently caused by intensity weighted mean particle diameter in case of DLS contrary to number weighted diameter obtained by TEM analysis [11]. More importantly, DLS proves that prepared NPs are not agglomerated, which is of crucial importance for evaluation of their bactericidal effects.

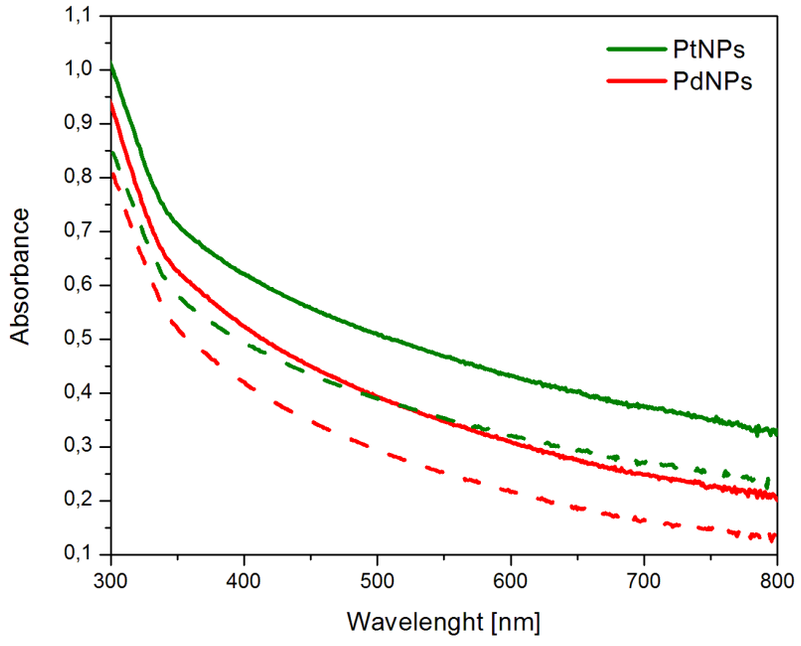

Figure 7. UV–Vis absorption spectra of Pt and Pd aqueous nanoparticle solutions. Dash lines represent UV–Vis spectra of Pt and Pd aqueous nanoparticle solutions stored for 3 months at laboratory conditions [21].

Formation and stability of metal NPs in aqueous colloidal solution were confirmed by UV–Vis spectroscopy. Figure 7 shows the UV–Vis spectra recorded from the Pd and PtNPs immediately after NPs preparation (solid lines) and after 3 months storage at laboratory conditions (dashed lines). It can be seen that apart from a distinct surface plasmon resonance (SPR) characteristic for other noble metal NPs (Au and Ag) [58], no distinctive SPR peaks occur in case of both Pd and PtNPs, which is in accordance with the earlier reports [89, 90]. Studied metal NPs exhibit increasing absorption toward shorter wavelengths [89, 91–93]. The course of dependence in case of both Pt and PdNPs indicates the presence of zerovalent metals in the solution [91]. Slight shift of the curves to lower absorbances at red region of visible spectrum (dashed lines) refers to mild agglomeration of individual particles in the solution after 3 months of storage. Bactericidal potency of various metal NPs has been previously reported [94–97]. It is known that their antimicrobial potency is governed by their size, composition, surface area, and charge [98, 99].

4. Antibacterial effects of noble metal nanoparticles

Antibacterial properties of Ag, Au, Pd, and PtNPs were examined using two bacterial strains, *E. coli* and *S. epidermidis*, frequently involved in infections associated with a biofilm formation. Demonstration of inhibition effect of $AgNP_{4–6}$ on *S. epidermidis* is shown in Figure 8. The growth of *E. coli* and *S. epidermidis* was completely inhibited in the presence of $AgNP_{4–6}$ after 24 h (for both 6 and 24 h incubated samples) when compared to the control samples (bacteria incubated in glycerol or physiological saline solution [PBS]), see Table 2 and Figure 8 [58].

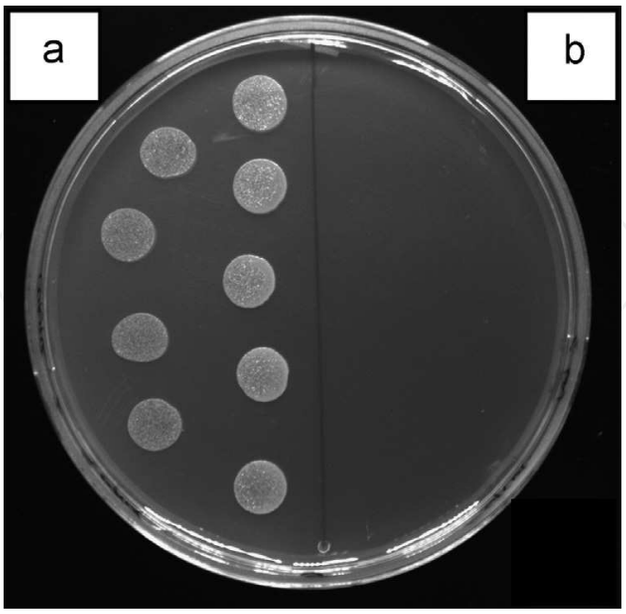

Figure 8. Photograph showing the inhibition effect of $AgNP_{4–6}$ on *Staphylococcus epidermidis* (a) positive control of bacterial colonies growing on agar plate, (b) bacterial sample treated with silver nanoparticles [58].

http://dx.doi.org/10.5772/61403

Bacteria	***E. coli***			***S. epidermidis***		
Growth Time **(h)**[a]	**24**	**30**	**48**	**24**	**30**	**48**
$AgNP_{4-6}$	○[b]	○	○	○	○	○
$AuNP_{4-6}$	●[c]	●	●	○	○	○
$AuNP_{9-12}$	●	●	●	○	○	○
Glycerol	●	●	●	○	○	○
PBS[d]	●	●	●	◐[e]	○	○

Table 2. Inhibitory effect of silver and gold nanoparticles against Gram-negative (*E. coli*) and Gram-positive (*S. epidermidis*) bacteria ([a]time length of bacterial growth on LB plates after inoculation, [b]an empty circle indicates inhibition effect, [c]a full circle indicates positive growth, [d]physiological saline solution, [e]a half full circle indicates 50 % growth) [58].

The growth inhibition of both bacterial strains was further maintained even after 30 and 48 h of growth, suggesting strong bactericidal activity of $AgNP_{4–6}$. This is in contrary to generally accepted fact that Gram-negative bacteria are more susceptible to the inhibitory action of silver [100] caused probably by more facile penetration of silver through their thinner cell wall. On contrary, any growth inhibition was observed toward *E. coli* neither in the presence of $AuNP_{4–6}$ nor in the presence of $AuNP_{9–12}$ during the whole experiment. Surprisingly, $AuNP_{4–6}$, but not $AuNP_{9–12}$, were able to inhibit the growth of *S. epidermidis* and the effect was preserved for whole tested period (48 h), when compared to control samples. The antibacterial action of Ag+ ions has been broadly reported so far [101], also AgNPs repeatedly showed their potency against bacteria [102]. Thus, our results (growth inhibition of both bacterial strains by $AgNP_{4–6}$) are in agreement with other groups results. Biocidal properties of AuNPs of similar size (5 nm) as prepared by our group (4–6 nm), were observed by Lima et al. [103]. Their AuNPs dispersed on zeolites were effective against Gram-negative *E. coli* and *Salmonella typhi* (90–95% growth inhibition). It has been reported that the antibacterial activity of AgNP is dependent on particle size and shape [104, 105]. Thus, it is very likely that also the size of AuNP plays significant role in the antimicrobial action.

Although there has been increased interest in studying bactericidal properties of noble metals over the past decades, only few have been reported on Pt and PdNPs. The inhibitory effect of one NPs concentration and four concentrations of bacteria was examined after 4 h in contact with NPs and 24 h of further post-incubation. From Figure 9, it is apparent that incubation of PdNPs with *E. coli* had pronounced effect on its growth up to 1 10^5 CFU per sample when compared to untreated control cells.

This remarkable antibacterial activity of Pd was diminished at higher bacterial concentrations ranging from 1 10^6 CFU per sample. Similar potency of PdNPs was observed against *S. epidermidis* (see Figure 9), even up to 1 10^6 CFU. Since PtNPs had very similar size as the first examined particles, the palladium ones, we expected comparable antimicrobial potential. Nevertheless, we detected only insignificant inhibition of bacterial growth induced by PtNPs at a concentration of 1 10^5 CFU of *E. coli* when compared to the control samples. Interestingly,

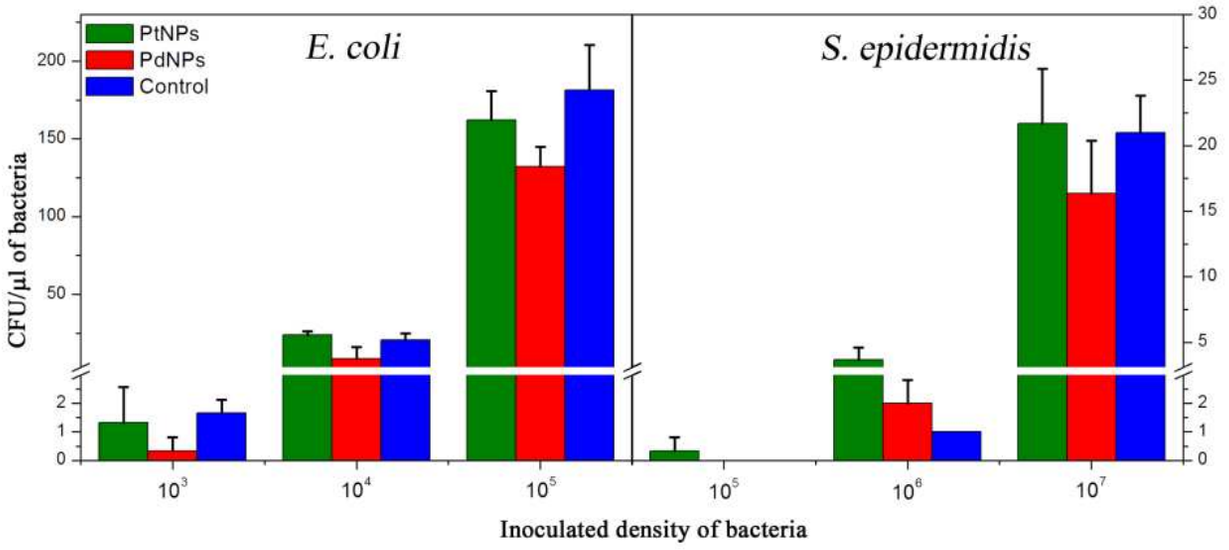

Figure 9. Inhibition effect of PtNPs and PdNPs toward bacterial strains of *E. coli* and *S. epidermidis* with different bacteria concentrations [21].

we did not observe any growth inhibition of *S. epidermidis* in the presence of PtNPs. More importantly, we even recorded slight stimulation of their growth.

5. Grafting of noble metal nanoparticles to plasma-activated polymer carriers

Polymer surface can be considered as the phase boundary between the bulk polymer and the ambient environment. The application of polymeric materials depends significantly on the boundaries' conditions. The most of polymeric materials, nevertheless, have chemically inert surface, mostly hydrophobic. Non-treated polymer surfaces exhibit very often poor performance in adhesion, coating, packaging, or colloid stabilization. [106–109].

During the past few decades, the modifications of polymer surface were under intensive research for applications in various fields of industry. Different improved techniques including chemical or physical enhancements were applied. Physical processes possess the advantage of surface interaction with radiation of electromagnetic waves, and oxidation with gases. On the contrary, chemical modifications use wet-treatment, such as blending. This part of manuscript is focused on the review of recent advances in surface grafting of polymer substrates which can be performed by the combination of physical and chemical processes [107, 110]. The advantages of grafting procedures in comparison to other procedures may be summarized to several points, such as controllable introduction of graft chains with a high density, the precise localization of graft chains to the surface with almost no change in bulk's surface properties. In contrast to physically coated polymer chains, covalent anchoring of graft

http://dx.doi.org/10.5772/61403

chains onto a polymer surface avoids their delamination and assures their long-term chemical stability [111].

Minimally four strategies can be used for creation of functionalized polymer surfaces with gold nanostructures: (i) "grafting from procedure" is based on polymer chain growth from small initiators connected to AuNPs [112, 113]. This procedure leads to a very dense polymer brush construction. Other methods are based on radical polymerization (LRP) [114] and atom-transfer radical polymerization (SI-ATRP) [115, 116] (ii) "grafting to" enables one-pot synthesis of AuNPs stabilized by sulphur-containing polymers [10, 117], and generally produces a sparser coverage [118] (iii) physisorption using block copolymer micelles (nanoreactors), water-soluble polymers, or star block copolymers [119, 120] (iv) "post-modification of pre-formed AuNPs". In this method, AuNPs are generated in the first stage through conventional methods such as Brust–Schiffrin synthesis, followed by the exchange or modification with polymers [121, 122].

This section is dedicated to description of two procedures of Au and AgNPs grafting on plasma-modified PET developed by our group. In the first procedure, Au and AgNPs were deposited on PET, beforehand grafted with biphenyl-4,4′-dithiol (BPD). In the second procedure, the Au and AgNPs (both denoted with*), beforehand grafted with BPD, were coated onto plasma-modified PET (see Figure 10).

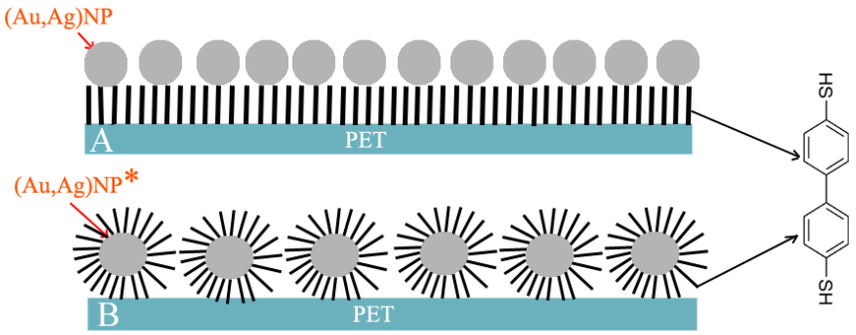

Figure 10. Scheme of PET modification: (A) plasma treatment, grafting with biphenyl-4,4′-dithiol (BPD) and then with AuNP or AgNP. (B) Plasma treatment, grafting with AuNP* or AgNP* covered with BPD [126].

In Figure 11, one can see the images of AuNPs obtained by TEM and HRTEM. It is evident that the AuNPs size is the same before and after BPD coating and their average diameter is 14.7 nm. Grafting with BPD does not lead to AuNPs aggregation, thanks to the presence of hydrophilic groups on the NP surface. It is known that the gold grows in a square *fcc* crystal structure with dominant plane (111) [123]. At higher HRTEM resolution (Figure 11C,E), it is seen that the AuNPs are in the form of decahedral particles. As a result of deficiency, real AuNPs should contain defects or be intrinsically strained [124]. In Figure 10E, gold atoms arranged in (111) plane are clearly seen. From Figure 11D, it is seen that some of the form of BPD-coated AuNPs differs from that of uncoated AuNPs and they are not in the form of decahedral particles due to the decrease of the surface tension [125]. It is apparent that the behavior of pristine AgNPs (AgNP in Figure 11F) and AgNPs modified with BPD (AgNP* in

Figure 11G) is significantly changed. AgNPs form uniform aggregates with nonspherical shape. On the contrary, AgNPs* form structures with spherical character which are well dispersed. Surface modification technique with BPD application does not result in AgNPs aggregation due to the presence of hydrophilic (-SH) and hydrophobic groups the nanoparticle's surface. The calculated diameters of AgNP and AgNP* were (55±10) and (45±10) nm, respectively [126].

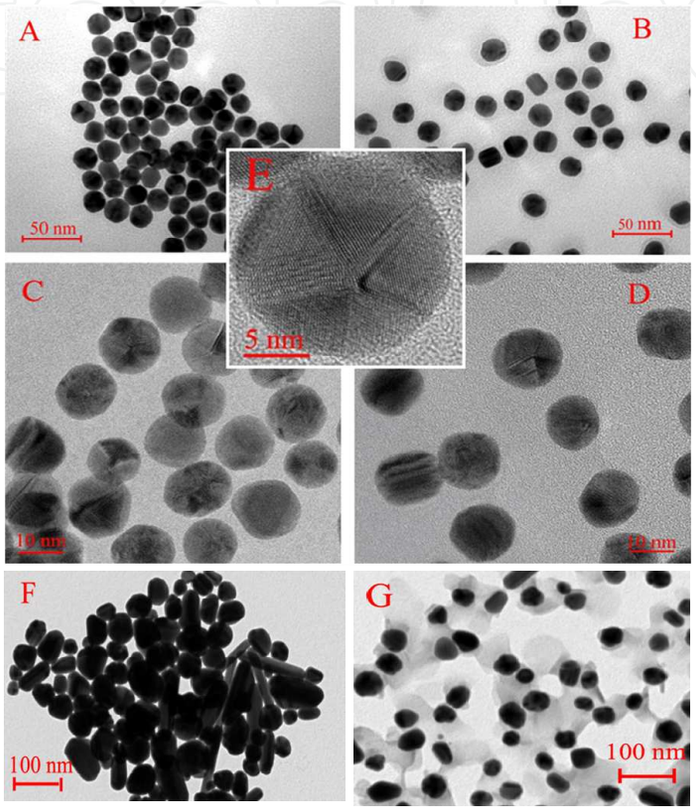

Figure 11. Images of the Au nanoparticles. TEM: (A) AuNPs and (B) AuNPs coated with dithiol (AuNP*). HRTEM: (C) AuNPs, (D) AuNPs coated with BPD (AuNP*), and (E) detail of AuNP; TEM images of the silver nanoparticles: (F) AgNP and (G) AgNPs coated with BPD (AgNP*) [125, 126].

Both (Au, Ag)NPs and (Au, Ag)NPs* in solution were characterized by UV–Vis spectroscopy (see Figure 12). The absorption spectrum of the AuNPs solution (see Figure 12A) shows a maximum around 521 nm, corresponding to the transverse plasmon oscillation band. The wavelength of the surface plasmon resonance (SPR) [127] corresponds well with the average diameter estimated from TEM images. SPR absorption wavelength is known to increase with nanoparticle size [124]. From Figure 12, it is obvious that the absorption maximum of AuNP* is shifted toward larger wave lengths. This finding is in accordance with the above mentioned fact that the BPD-coated AuNPs (AuNPs*) exhibit enlarged surface [128]. The UV–Vis absorption spectra of AgNPs and AgNPs* suspensions (Figure 12B) exhibit well-defined plasmon bands at about 455 and 413 nm, which is characteristic of nano-sized silver [31, 97, 129]. Observed wavelengths correspond well with average diameters of AgNPs estimated from TEM images (Figure 11F,G).

http://dx.doi.org/10.5772/61403

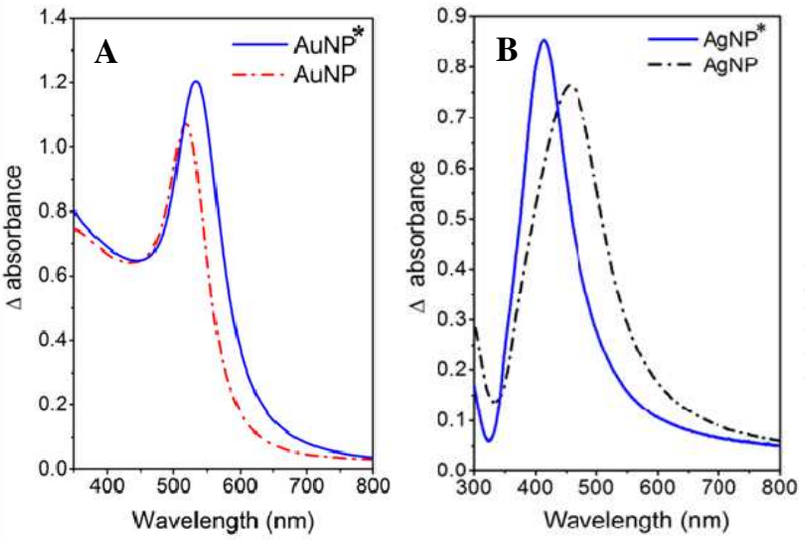

Figure 12. UV–Vis spectra of water solutions of (A) AuNPs (red) and AuNPs covered with BPD (AuNP*, blue); (B) AgNPs (black) and AgNPs covered with BPD (AgNP*, blue) [125, 126].

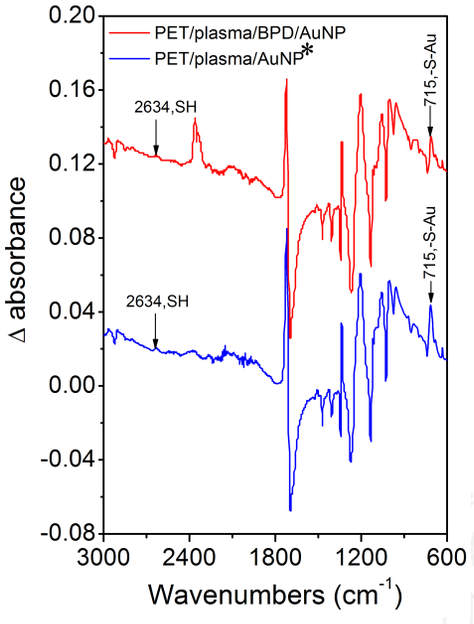

Figure 13. Differential FTIR spectra of plasma-treated PET grafted with BPD and then with AuNPs (PET/plasma/BPD/AuNP, red) or plasma-treated PET and grafted with AuNPs covered with BPD (PET/plasma/AuNP*, blue) [125].

Differential FTIR spectroscopy was used for the characterization of pristine PET, plasma-treated PET, and PET grafted with BPD and AuNPs using both techniques described above. Typical difference FTIR spectra are shown in Figure 13. The band at 2634 cm^{-1} corresponds to residual dithiol group. The band at 715 cm^{-1} corresponds to the –S–Au group. So that, the FTIR measurement proves that the AuNPs, deposited using both procedures examined, are chemically bound to the plasma-activated PET surface.

XPS analysis was used to monitor the change in the surface chemical composition after subsequent preparation steps. Element concentration of C, O, S, and Au on the surface of all samples (using both grafting techniques) is summarized in Table 3. After the plasma treatment, the PET surface is oxidized dramatically. The polymer oxidation after the plasma treatment and creation of oxygen-containing groups (C–O ~ 286.0 eV, O–C=O ~ 288.8 eV) at the polymer surface is well known [130]. Polymer chain is characterized by the C1s component centered at 284.7 eV due to C–C group. There is a change in the contribution of the shake-up satellite 290.9 eV due to the attachment of aromatic species (BPD) to the plasma-treated PET, see references [125, 131]. After grafting of plasma-treated PET with BPD, the oxygen concentration decreases dramatically. The attachment of BPD to the surface of PET (PET/BPD) was evidenced by the detection of the sulphur with concentration of 5.7 at. %. The concentration of bonded AuNP and AuNP* varies from 0.1 to 0.02 at. %, respectively. Atomic concentrations of C(1s), O(1s), S(2p), and Ag(3d) in pristine, plasma-modified PET and after grafting with BPD and silver nanoparticles are summarized in Table 3. After the next grafting procedure realized with AgNP and AgNP* particles, the concentration of sulphur decreased and silver was confirmed for the PET/plasma/BPD/AgNP samples, which indicates the presence of AgNPs on the surface of treated PET. In the case of PET/plasma/AgNP* samples, the silver concentration is presumably below the detection limit of XPS method. However, the evidence of successful AgNP* attachment was confirmed by the presence of sulphur on the treated surface.

Sample	**Element concentration (at. %)**			
	C(1s)	O(1s)	S(2p)	Au(4f)
PET	72.5	27.5	-	-
PET/plasma	29.0	71.0	-	-
PET/plasma/BPD	75.4	18.9	5.7	-
PET/plasma/BPD/AuNP	72.6	24.6	2.7	0.1
PET/plasma/AuNP*	72.2	26.4	1.4	0.02

Table 3. Atomic concentration of C, O, S, and Au measured with XPS in surface polymer layer for: pristine (PET), plasma exposed (PET/plasma), plasma exposed and grafted with BPD (PET/plasma/BPD) and then grafted with AuNP (PET/plasma/BPD/AuNP) and grafted with AuNP* (PET/plasma/AuNP*) 4 days after the exposure [125].

It is known that the thiol groups bond to double bonds created on surface by plasma treatment by free radical chain mechanism [132]. Radicals created after plasma activation of PET are located mainly at heteroatoms (e.g., oxygen of ester or hydroxyl group). Therefore, these radicals are stable and do not stabilize by creation of double bonds on surface [133]. In our previous study [134], it has been proved the amount of free radicals created on PET surface modified by plasma is very low. That is the reason why more double bonds are not available on PET, and therefore the amount of bonded thiol groups is not much higher [125, 126].

6. Conclusions

This chapter attempts to provide a comprehensive insight into the problems of new techniques of preparation of noble metal NPs. It summarizes the basic information about the elementary

http://dx.doi.org/10.5772/61403

characteristics and technology of preparation of those man-made materials. The introduction gives some basic information on the history of development in this area, especially in terms of dimensionality of metal nanostructures and their possible applications. General overview is supported by the specific research of the author team in this field. Presented findings support the hypothesis that Au, Ag, Pd, and PtNPs can be prepared in a simple and cost-effective manner and are suitable for formulation of new types of bactericidal materials. Presented approach is based on temperature control of capturing media during the sputtering deposition process into propane-1,2,3-triol, allowing targeted variation of NPs size. Bactericidal action of such synthesized NPs was examined against two common pollutants (*E. coli* and *S. epidermidis*). While $AgNP_{4–6}$ exhibit strong potential to completely inhibit both bacterial strains after 24 h, AuNPs showed pronounced inhibition selectivity regarding the specific NP size. Regardless of AuNP size, any growth inhibition of *E. coli* was observed. Contrary to that, $AuNP_{4–6}$ were able to inhibit the growth of *S. epidermidis*. We have also illustrated a significant difference in biological activities of Pt and PdNPs. More specifically, PdNPs exhibited considerable inhibitory potential against both *E. coli* and *S. epidermidis*, which was in contrast to ineffective PtNPs. Those findings indicate that palladium has high potential to combat both Gram-positive and Gram-negative bacterial strains. Understanding of nanoparticle–bacteria interactions is a key issue in their potential applications in clinics on everyday basis. Observed discrepancy in bactericidal action between Pt and Pd nanoparticles could be attributed to different size of individual particles. Finally, we have introduced procedures for PET surface coating with noble metal nanoparticles. The techniques were based on activation of PET surface with Ar plasma discharge and consequent application of dithiol as binding reagent between Au and Ag nanoparticles and plasma-treated PET. The introduction of gold and silver nanoparticle–thiol layer on the activated PET surface was confirmed with XPS analysis. Higher concentration of Au and AgNPs was achieved by deposition on PET grafted beforehand with dithiol.

Acknowledgements

Financial support of this work under the GACR projects Nos. 14-18131S, 14-18149P, and 13-06609S is gratefully acknowledged.

Author details

Jakub Siegel*, Alena Řezníčková, Petr Slepička and Václav Švorčík

*Address all correspondence to: jakub.siegel@vscht.cz

Department of Solid State Engineering, University of Chemistry and Technology Prague, Prague, Czech Republic

References

[1] Zhou J, Ralston J, Sedev R, Beattie DA. Functionalized gold nanoparticles: synthesis, structure and colloid stability. J Colloid Interface Sci 2009;331:251–62. 10.1016/j.jcis.2008.12.002

[2] Zhang L, Wang E. Metal nanoclusters: new fluorescent probes for sensors and bioimaging. Nano Today 2014;9:132–57. 10.1016/j.nantod.2014.02.010

[3] Ghosh P, Han G, De M, Kim CK, Rotello VM. Gold nanoparticles in delivery applications. Adv Drug Delivery Rev 2008;60:1307–15. 10.1016/j.addr.2008.03.016

[4] Kamat PV. Photophysical, photochemical and photocatalytic aspects of metal nanoparticles. J Phys Chem B 2002;106:7729–44. 10.1021/jp0209289

[5] Cheng H-W, Luo J, Zhong C-J. An aggregative growth process for controlling size, shape and composition of metal, alloy and core-shell nanoparticles toward desired bioapplications. J Mater Chem B 2014;2:6904–16. 10.1039/c4tb00962b

[6] Sahoo GP, Basu S, Samanta S, Misra A. Microwave-assisted synthesis of anisotropic gold nanocrystals in polymer matrix and their catalytic activities. J Exp Nanosci 2015;10:690–702. 10.1080/17458080.2013.877163

[7] El Roustom B, Foti G, Comninellis C. Preparation of gold nanoparticles by heat treatment of sputter deposited gold on boron-doped diamond film electrode. Electrochem Commun 2005;7:398–405. 10.1016/j.elecom.2005.02.014

[8] Turkevich J, Stevenson PC, Hillier J. A study of the nucleation and growth processes in the synthesis of colloidal gold. Discuss Faraday Soc 1951:55.

[9] Grzelczak M, Perez-Juste J, Mulvaney P, Liz-Marzan LM. Shape control in gold nanoparticle synthesis. Chem Soc Rev 2008;37:1783-1791. 10.1039/b711490g

[10] Hussain I, Graham S, Wang ZX, Tan B, Sherrington DC, Rannard SP, Cooper AI, Brust M. Size-controlled synthesis of near-monodisperse gold nanoparticles in the 1-4 nm range using polymeric stabilizers. J Am Chem Soc 2005;127:16398–9. 10.1021/ja055321v

[11] Uskokovic V. Dynamic light scattering based microelectrophoresis: main prospects and limitations. J Dispersion Sci Technol 2012;33:1762–86. 10.1080/01932691.2011.625523

[12] Zhang Q, Tan YN, Xie J, Lee JY. Colloidal synthesis of plasmonic metallic nanoparticles. Plasmonics 2009;4:9–22. 10.1007/s11468-008-9067-x

[13] Migowski P, Dupont J. Catalytic applications of metal nanoparticles in imidazolium ionic liquids. Chem Eur J 2007;13:32–39. 10.1002/chem.200601438

[14] Soto-Aquino D, Rinaldi C. Nonlinear energy dissipation of magnetic nanoparticles in oscillating magnetic fields. J Magn Magn Mater 2015;393:46–55.

[15] Zhang X, Wu F-G, Liu P, Wang H-Y, Gu N, Chen Z. Synthesis of ultrastable and multifunctional gold nanoclusters with enhanced fluorescence and potential anticancer drug delivery application. J Colloid Interface Sci 2015;455:6–15. 10.1016/j.jcis.2015.05.029

[16] Joshi MK, Pant HR, Liao N, Kim JH, Kim HJ, Park CH, Kim CS. In-situ deposition of silver-iron oxide nanoparticles on the surface of fly ash for water purification. J Colloid Interface Sci 2015;453:159–68. 10.1016/j.jcis.2015.04.044

[17] Taaber T, Enok AE, Joost U, Oras S, Jaervekuelg M, Lohmus R, Maeeorg U, Saal K. Tribological properties of protic ionic liquid and functionalized copper oxide nanoparticles as additives to base oil. Mechanika 2015:148–153. 10.5755/j01.mech.21.2.11723

[18] Vallejos S, Gracia I, Bravo J, Figueras E, Hubalek J, Cane C. Detection of volatile organic compounds using flexible gas sensing devices based on tungsten oxide nanostructures functionalized with Au and Pt nanoparticles. Talanta 2015;139:27–34. 10.1016/j.talanta.2015.02.034

[19] Melo Ferreira DC, Giordano GF, dos Santos Penteado Soares CC, Afonso de Oliveira JF, Mendes RK, Piazzetta MH, Gobbi AL, Cardoso MB. Optical paper-based sensor for ascorbic acid quantification using silver nanoparticles. Talanta 2015;141:188–94. 10.1016/j.talanta.2015.03.067

[20] Kannan R, Kim AR, Lee H-K, Yoo DJ. Coordinated fast synthesis of electrocatalytic palladium nanoparticles decorated graphene oxide nanocomposite for fuel cell applications. J Nanosci Nanotechnol 2015;15:5711–17. 10.1166/jnn.2015.10042

[21] Staszek M, Siegel J, Kolarova K, Rimpelova S, Svorcik V. Formation and antibacterial action of Pt and Pd nanoparticles sputtered into liquid. Micro Nano Lett 2014;9:778–81. 10.1049/mnl.2014.0345

[22] Siegel J, Kvitek O, Lyutakov O, Reznickova A, Svorcik V. Low pressure annealing of gold nanostructures. Vacuum 2013;98:100–5. 10.1016/j.vacuum.2013.03.019

[23] Yang X. Nano- and microparticle-based imaging of cardiovascular interventions: overview. Radiology 2007;243:340–7. 10.1148/radiol.2432060307

[24] Lanza GM, Winter PM, Caruthers SD, Hughes MS, Cyrus T, Marsh JN, Neubauer AM, Partlow KC, Wickline SA. Nanomedicine opportunities for cardiovascular disease with perfluorocarbon nanoparticles. Nanomed 2006;1:321–9. 10.2217/17435889.1.3.321

[25] Brust M, Walker M, Bethell D, Schiffrin DJ, Whyman R. Synthesis of thiol-derivatized gold nanoparticles in a 2-phase liquid-liquid system. J Chem Soc Chem Comm 1994:801–2. 10.1039/c39940000801

[26] Sahiner N. Soft and flexible hydrogel templates of different sizes and various functionalities for metal nanoparticle preparation and their use in catalysis. Prog Polym Sci 2013;38:1329–56. 10.1016/j.progpolymsci.2013.06.004

[27] Sahiner N, Singh M. In situ micro/nano-hydrogel synthesis from acrylamide derivates with lecithin organogel system. Polymer 2007;48:2827–34. 10.1016/j.polymer.2007.01.005

[28] Jayamurugan G, Umesh CP, Jayaraman N. Preparation and catalytic studies of palladium nanoparticles stabilized by dendritic phosphine ligand-functionalized silica. J Mol Catal A-Chem 2009;307:142–8. 10.1016/j.molcata.2009.03.020

[29] Costi R, Saunders AE, Banin U. Colloidal hybrid nanostructures: a new type of functional materials. Angew Chem-Int Edit 2010;49:4878–97. 10.1002/anie.200906010

[30] Ahn H, Park MJ. Facile one-pot synthesis of functional gold nanoparticle-polymer hybrids using ionic block copolymers as a nanoreactor. Macromol Rapid Commun 2011;32:1790–7. 10.1002/marc.201100449

[31] Siegel J, Kvitek O, Ulbrich P, Kolska Z, Slepicka P, Svorcik V. Progressive approach for metal nanoparticle synthesis. Mater Lett 2012;89:47–50. 10.1016/j.matlet.2012.08.048

[32] Metin O, Dinc M, Eren ZS, Ozkar S. Silica embedded cobalt(0) nanoclusters: efficient, stable and cost effective catalyst for hydrogen generation from the hydrolysis of ammonia borane. Int J Hydrogen Energy 2011;36:11528–35. 10.1016/j.ijhydene.2011.06.057

[33] Sutton A, Franc G, Kakkar A. Silver metal nanoparticles: facile dendrimer-assisted size-controlled synthesis and selective catalytic reduction of chloronitrobenzenes. J Polymer Sci Part A Polymer Chem 2009;47:4482–93. 10.1002/pola.23501

[34] Li Y, Pan Y, Zhu L, Wang Z, Su D, Xue G. Facile and controlled fabrication of functional gold nanoparticle-coated polystyrene composite particle. Macromol Rapid Commun 2011;32:1741–47. 10.1002/marc.201100377

[35] Goyal A, Kumar A, Patra PK, Mahendra S, Tabatabaei S, Alvarez PJJ, John G, Ajayan PM. In situ synthesis of metal nanoparticle embedded free standing multifunctional PDMS films. Macromol Rapid Commun 2009;30:1116–22. 10.1002/marc.200900174

[36] Suzuki D, Kawaguchi H. Gold nanoparticle localization at the core surface by using thermosensitive core-shell particles as a template. Langmuir 2005;21:12016–24. 10.1021/la0516882

[37] Lu Y, Mei Y, Schrinner M, Ballauff M, Moeller MW. In situ formation of Ag nanoparticles in spherical polyacrylic acid brushes by UV irradiation. J Phys Chem C 2007;111:7676–81. 10.1021/jp070973m

[38] Konishi N, Fujibayashi T, Tanaka T, Minami H, Okubo M. Effects of properties of the surface layer of seed particles on the formation of golf ball-like polymer particles by

seeded dispersion polymerization. Polym J (Tokyo, Jpn) 2010;42:66–71. 10.1038/pj.2009.313

[39] Frattini A, Pellegri N, Nicastro D, de Sanctis O. Effect of amine groups in the synthesis of Ag nanoparticles using aminosilanes. Mater Chem Phys 2005;94:148–52. 10.1016/j.matchemphys.2005.04.023

[40] Liu H, Wang C, Gao Q, Liu X, Tong Z. Fabrication of novel core-shell hybrid alginate hydrogel beads. Int J Pharm 2008;351:104–12. 10.1016/j.ijpharm.2007.09.019

[41] Butun S, Sahiner N. A versatile hydrogel template for metal nano particle preparation and their use in catalysis. Polymer 2011;52:4834–40. 10.1016/j.polymer.2011.08.021

[42] Nguyen LH, Kudva AK, Saxena NS, Roy K. Engineering articular cartilage with spatially-varying matrix composition and mechanical properties from a single stem cell population using a multi-layered hydrogel. Biomaterials 2011;32:6946–52. 10.1016/j.biomaterials.2011.06.014

[43] Nuttelman CR, Rice MA, Rydholm AE, Salinas CN, Shah DN, Anseth KS. Macromolecular monomers for the synthesis of hydrogel niches and their application in cell encapsulation and tissue engineering. Prog Polym Sci 2008;33:167–79. 10.1016/j.progpolymsci.2007.09.006

[44] Nicodemus GD, Bryant SJ. Cell encapsulation in biodegradable hydrogels for tissue engineering applications. Tissue Eng Part B Rev 2008;14:149–65. 10.1089/ten.teb.2007.0332

[45] Ozay O, Aktas N, Sahiner N. Hydrogels as a potential chromatographic system: absorption, speciation, and separation of chromium species from aqueous media. Sep Sci Technol 2011;46:1450–61. 10.1080/01496395.2011.560918

[46] Ye GX, Zhang QR, Feng CM, Ge HL, Jiao ZK. Structural and electrical properties of a metallic rough-thin-film system deposited on liquid substrates. Phys Rev B. 1996;54:14754–7. 10.1103/PhysRevB.54.14754

[47] Ye GX, Geng CM, Zhang ZR, Ge HL, Zhang XJ. Structural and critical behaviors of ag rough films deposited on liquid substrates. Chin Phys Lett 1996;13:772–4. 10.1088/0256-307x/13/10/016

[48] Wender H, de Oliveira LF, Feil AF, Lissner E, Migowski P, Meneghetti MR, Teixeira SR, Dupont J. Synthesis of gold nanoparticles in a biocompatible fluid from sputtering deposition onto castor oil. Chem Commun 2010;46:7019–21. 10.1039/c0cc01353f

[49] da Silva EC, da Silva MGA, Meneghetti SMP, Machado G, Alencar MARC, Hickmann JM, Meneghetti MR. Synthesis of colloids based on gold nanoparticles dispersed in castor oil. J Nanoparticle Res 2008;10:201–8. 10.1007/s11051-008-9483-z

[50] Wender H, Goncalves RV, Feil AF, Migowski P, Poletto FS, Pohlmann AR, Dupont J, Teixeira SR. Sputtering onto liquids: from thin films to nanoparticles. J Phys Chem C 2011;115:16362–7. 10.1021/jp205390d

[51] Dupont J, de Souza RF, Suarez PAZ. Ionic liquid (molten salt) phase organometallic catalysis. Chem Rev 2002;102:3667–91. 10.1021/cr010338r

[52] Wender H, Migowski P, Feil AF, Teixeira SR, Dupont J. Sputtering deposition of nanoparticles onto liquid substrates: recent advances and future trends. Coord Chem Rev 2013;257:2468–83. 10.1016/j.ccr.2013.01.013

[53] Antonietti M, Kuang DB, Smarsly B, Yong Z. Ionic liquids for the convenient synthesis of functional nanoparticles and other inorganic nanostructures. Angew Chem-Int Edit 2004;43:4988–92. 10.1002/anie.200460091

[54] Wender H, de Oliveira LF, Migowski P, Feil AF, Lissner E, Prechtl MHG, Teixeira SR, Dupont J. Ionic liquid surface composition controls the size of gold nanoparticles prepared by sputtering deposition. J Phys Chem C 2010;114:11764–8. 10.1021/jp102231x

[55] Migowski P, Zanchet D, Machado G, Gelesky MA, Teixeira SR, Dupont J. Nanostructures in ionic liquids: correlation of iridium nanoparticles' size and shape with imidazolium salts' structural organization and catalytic properties. Phys Chem Chem Phys 2010;12:6826–33. 10.1039/b925834e

[56] Redel E, Thomann R, Janiak C. Use of ionic liquids (ILs) for the IL-anion size-dependent formation of Cr, Mo and W nanoparticles from metal carbonyl M(CO)(6) precursors. Chem Commun 2008:1789–91. 10.1039/b718055a

[57] Redel E, Thomann R, Janiak C. First correlation of nanoparticle size-dependent formation with the ionic liquid anion molecular volume. Inorg Chem 2008;47:14–6. 10.1021/ic702071w

[58] Siegel J, Kolarova K, Vosmanska V, Rimpelova S, Leitner J, Svorcik V. Antibacterial properties of green-synthesized noble metal nanoparticles. Mater Lett 2013;113:59–62. 10.1016/j.matlet.2013.09.047

[59] Silver S, Phung LT. Bacterial heavy metal resistance: new surprises. Annu Rev Microbiol 1996;50:753–89. 10.1146/annurev.micro.50.1.753

[60] Samuel U, Guggenbichler JP. Prevention of catheter-related infections: the potential of a new nano-silver impregnated catheter. Int J Antimicrob Agents 2004;23:S75–8. 10.1016/j.ijantimicag.2003.12.004

[61] Catauro M, Raucci MG, De Gaetano F, Marotta A. Antibacterial and bioactive silver-containing Na2O center dot CaO center dot 2SiO(2) glass prepared by sol-gel method. J Mater Sci Mater Med 2004;15:831–7. 10.1023/b:jmsm.0000032825.51052.00

[62] Lee W, Kim K-J, Lee DG. A novel mechanism for the antibacterial effect of silver nanoparticles on Escherichia coli. BioMetals 2014;27:1191–201. 10.1007/s10534-014-9782-z

[63] Ansari MA, Khan HM, Khan AA, Ahmad MK, Mahdi AA, Pal R, Cameotra SS. Interaction of silver nanoparticles with Escherichia coli and their cell envelope biomolecules. J Basic Microbiol 2014;54:905–15. 10.1002/jobm.201300457

[64] Mikhlin Y, Karacharov A, Likhatski M, Podlipskaya T, Zubavichus Y, Veligzhanin A, Zaikovski V. Submicrometer intermediates in the citrate synthesis of gold nanoparticles: new insights into the nucleation and crystal growth mechanisms. J Colloid Interface Sci 2011;362:330–6. 10.1016/j.jcis.2011.06.077

[65] Wagner J, Kohler JM. Continuous synthesis of gold nanoparticles in a microreactor. Nano Lett 2005;5:685–91. 10.1021/nl050097t

[66] Zhang A, Liu M, Liu M, Xiao Y, Li Z, Chen J, Sun Y, Zhao J, Fang S, Jia D, Li F. Homogeneous Pd nanoparticles produced in direct reactions: green synthesis, formation mechanism and catalysis properties. J Mater Chem A 2014;2:1369–74. 10.1039/c3ta14299j

[67] Liu Y, Liu L, Yuan M, Guo R. Preparation and characterization of casein-stabilized gold nanoparticles for catalytic applications. Colloids Surfaces Physicochem Eng Asp 2013;417:18–25. 10.1016/j.colsurfa.2012.08.050

[68] Doyen M, Bartik K, Bruylants G. UV-Vis and NMR study of the formation of gold nanoparticles by citrate reduction: Observation of gold-citrate aggregates. J Colloid Interface Sci 2013;399:1–5. 10.1016/j.jcis.2013.02.040

[69] De S, Kundu R, Biswas A. Synthesis of gold nanoparticles in niosomes. J Colloid Interface Sci 2012;386:9–15. 10.1016/j.jcis.2012.06.073

[70] Wangoo N, Bhasin KK, Mehta SK, Suri CR. Synthesis and capping of water-dispersed gold nanoparticles by an amino acid: Bioconjugation and binding studies. J Colloid Interface Sci 2008;323:247–54. 10.1016/j.jcis.2008.04.043

[71] Hori T, Nagata K, Iwase A, Hori F. Synthesis of Cu nanoparticles using gamma-ray irradiation reduction method. Japanese Journal of Applied Physics. 2014;53. 10.7567/jjap.53.05fc05

[72] Yokoyama S, Takahashi H, Itoh T, Motomiya K, Tohji K. Synthesis of metallic Cu nanoparticles by controlling Cu complexes in aqueous solution. Advanced Powder Technology. 2014;25:999-1006. 10.1016/j.apt.2014.01.024

[73] Bankar A, Joshi B, Kumar AR, Zinjarde S. Banana peel extract mediated synthesis of gold nanoparticles. Colloids and Surfaces B-Biointerfaces. 2010;80:45-50. 10.1016/j.colsurfb.2010.05.029

[74] Bankar A, Joshi B, Kumar AR, Zinjarde S. Banana peel extract mediated novel route for the synthesis of palladium nanoparticles. Mater Lett 2010;64:1951–53. 10.1016/j.matlet.2010.06.021

[75] Bankar A, Joshi B, Kumar AR, Zinjarde S. Banana peel extract mediated novel route for the synthesis of silver nanoparticles. Colloids Surfaces A Physicochem Eng Aspects 2010;368:58–63. 10.1016/j.colsurfa.2010.07.024

[76] Das RK, Sharma P, Nahar P, Bora U. Synthesis of gold nanoparticles using aqueous extract of Calotropis procera latex. Mater Lett 2011;65:610–3. 10.1016/j.matlet.2010.11.040

[77] Ren F, He X, Wang K, Yin J. Biosynthesis of gold nanoparticles using catclaw buttercup (Radix Ranunculi Ternati) and evaluation of its colloidal stability. J Biomed Nanotechnol 2012;8:586–93. 10.1166/jbn.2012.1417

[78] Im H-J, Lee BC, Yeon J-W. Preparation and characterization of Ag nanoparticle-embedded blank and ligand-anchored silica gels. J Nanosci Nanotechnol 2013;13:7643–7. 10.1166/jnn.2013.7824

[79] Sarkar P, Bhui DK, Bar H, Sahoo GP, De SP, Misra A. Synthesis and photophysical study of silver nanoparticles stabilized by unsaturated dicarboxylates. J Lumin 2009;129:704–9. 10.1016/j.jlumin.2009.02.002

[80] Mirkin CA, Taton TA. Materials chemistry – semiconductors meet biology. Nature 2000;405:626–7. 10.1038/35015190

[81] Sarkar A, Kapoor S, Mukherjee T. Synthesis and characterisation of silver nanoparticles in viscous solvents and its transfer into non-polar solvents. Res Chem Intermed 2010;36:411–421. 10.1007/s11164-010-0151-4

[82] Daniel MC, Astruc D. Gold nanoparticles: assembly, supramolecular chemistry, quantum-size-related properties, and applications toward biology, catalysis, and nanotechnology. Chem Rev 2004;104:293–346. 10.1021/cr030698+

[83] Li X, Jiang L, Zhan Q, Qian J, He S. Localized surface plasmon resonance (LSPR) of polyelectrolyte-functionalized gold-nanoparticles for bio-sensing. Colloids Surfaces APhysicochem Eng Aspects 2009;332:172–9. 10.1016/j.colsurfa.2008.09.009

[84] Link S, El-Sayed MA. Size and temperature dependence of the plasmon absorption of colloidal gold nanoparticles. J Phys Chem B 1999;103:4212–7. 10.1021/jp984796o

[85] Varkey AJ, Fort AF. Some optical properties of silver peroxide (Ago) and silver-oxide (AG2O) films produced by chemical bath deposition. Sol Energy Mater Sol Cells 1993;29:253–9. 10.1016/0927-0248(93)90040-a

[86] Park J, Joo J, Kwon SG, Jang Y, Hyeon T. Synthesis of monodisperse spherical nanocrystals. Angew Chem-Int Edit. 2007;46:4630–60. 10.1002/anie.200603148

[87] Cabrini S, Kawata S. Nanofabrication Handbook. Boca Raton: Taylor&Francis; 2012. 546 p.

[88] Baalousha M, Ju-Nam Y, Cole PA, Gaiser B, Fernandes TF, Hriljac JA, Jepson MA, Stone V, Tyler CR, Lead JR. Characterization of cerium oxide nanoparticles Part 1: size measurements. Environ Toxicol Chem 2012;31:983–93. 10.1002/etc.1785

[89] Chen L, Zhao W, Jiao W, He X, Wang J, Zhang Y. Characterization of Ag/Pt core-shell nanoparticles by UV-vis absorption, resonance light-scattering techniques. Spectrochim Acta Part A Molecul Biomolecul Spectrosc 2007;68:484–90. 10.1016/j.saa.2006.12.014

[90] Patel K, Kapoor S, Dave DP, Mukherjee T. Synthesis of Pt, Pd, Pt/Ag and Pd/Ag nanoparticles by microwave-polyol method. J Chem Sci (Bangalore, India). 2005;117:311–6. 10.1007/bf02708443

[91] Guo L, Bai J, Li C, Meng Q, Liang H, Sun W, Li H, Liu H. A novel catalyst containing palladium nanoparticles supported on PVP composite nanofiber films: synthesis, characterization and efficient catalysis. Appl Surf Sci 2013;283:107–14. 10.1016/j.apsusc.2013.06.046

[92] Kalbasi RJ, Negandari M. Synthesis and characterization of mesoporous poly(N-vinyl-2-pyrrolidone) containing palladium nanoparticles as a novel heterogeneous organocatalyst for Heck reaction. J Mol Struct 2014;1063:259–68. 10.1016/j.molstruc.2014.01.071

[93] Vinod VTP, Saravanan P, Sreedhar B, Devi DK, Sashidhar RB. A facile synthesis and characterization of Ag, Au and Pt nanoparticles using a natural hydrocolloid gum kondagogu (Cochlospermum gossypium). Colloids and Surfaces B-Biointerfaces. 2011;83:291–8. 10.1016/j.colsurfb.2010.11.035

[94] Adams CP, Walker KA, Obare SO, Docherty KM. Size-dependent antimicrobial effects of novel palladium nanoparticles. PLoS One 2014;9:1–6. 10.1371/journal.pone.0085981

[95] Panacek A, Kvitek L, Prucek R, Kolar M, Vecerova R, Pizurova N, Sharma VK, Nevecna Tj, Zboril R. Silver colloid nanoparticles: Synthesis, characterization, and their antibacterial activity. J Phys Chem B 2006;110:16248–53. 10.1021/jp063826h

[96] Rai M, Yadav A, Gade A. Silver nanoparticles as a new generation of antimicrobials. Biotechnol Adv 2009;27:76–83. 10.1016/j.biotechadv.2008.09.002

[97] Kim JS, Kuk E, Yu KN, Kim J-H, Park SJ, Lee HJ, Kim SH, Park YK, Park YH, Hwang C-Y, Kim Y-K, Lee Y-S, Jeong DH, Cho M-H. Antimicrobial effects of silver nanoparticles. Nanomed Nanotechnol Biol Med 2007;3:95–101. 10.1016/j.nano.2006.12.001

[98] Nel A, Xia T, Madler L, Li N. Toxic potential of materials at the nanolevel. Science 2006;311:622–7. 10.1126/science.1114397

[99] Singh S, Nalwa HS. Nanotechnology and health safety - Toxicity and risk assessments of nanostructured materials on human health. J Nanosci Nanotechnol 2007;7:3048–70. 10.1166/jnn.2007.922

[100] Jung WK, Koo HC, Kim KW, Shin S, Kim SH, Park YH. Antibacterial activity and mechanism of action of the silver ion in Staphylococcus aureus and Escherichia coli. Appl Environ Microbiol 2008;74:2171–8. 10.1128/aem.02001-07

[101] Klaus T, Joerger R, Olsson E, Granqvist CG. Silver-based crystalline nanoparticles, microbially fabricated. Proc Natl Acad Sci U S A 1999;96:13611–4. 10.1073/pnas.96.24.13611

[102] Raffi M, Hussain F, Bhatti TM, Akhter JI, Hameed A, Hasan MM. Antibacterial characterization of silver nanoparticles against E. coli ATCC-15224. J Mater Sci Technol 2008;24:192–6.

[103] Lima E, Guerra R, Lara V, Guzman A. Gold nanoparticles as efficient antimicrobial agents for Escherichia coli and Salmonella typhi. Chem Cent J 2013;7:1–5. 10.1186/1752-153x-7-11

[104] Darroudi M, Ahmad MB, Mashreghi M. Gelatinous silver colloid nanoparticles: synthesis, characterization, and their antibacterial activity. J Optoelectron Adv Mater 2014;16:182–7.

[105] Pal S, Tak YK, Song JM. Does the antibacterial activity of silver nanoparticles depend on the shape of the nanoparticle? A study of the gram-negative bacterium Escherichia coli. Appl Environ Microbiol 2007;73:1712–20. 10.1128/aem.02218-06

[106] Ozdemir M, Yurteri CU, Sadikoglu H. Physical polymer surface modification methods and applications in food packaging polymers. Crit Rev Food Sci Nutr 1999;39:457–77. 10.1080/10408699991279240

[107] Huang X, Jiang P, Yin Y. Nanoparticle surface modification induced space charge suppression in linear low density polyethylene. Appl Phys Lett 2009;95:1–6. 10.1063/1.3275732

[108] Jacobs T, Morent R, De Geyter N, Dubruel P, Leys C. Plasma surface modification of biomedical polymers: influence on cell-material interaction. Plasma Chem Plasma Process 2012;32:1039–73. 10.1007/s11090-012-9394-8

[109] Yoshida S, Hagiwara K, Hasebe T, Hotta A. Surface modification of polymers by plasma treatments for the enhancement of biocompatibility and controlled drug release. Surf Coat Technol 2013;233:99–107. 10.1016/j.surfcoat.2013.02.042

[110] Zhang T, Wu Y, Pan X, Zheng Z, Ding X, Peng Y. An approach for the surface functionalized gold nanoparticles with pH-responsive polymer by combination of RAFT and click chemistry. Eur Polym J 2009;45:1625–33. 10.1016/j.eurpolymj.2009.03.016

[111] Kato K, Uchida E, Kang ET, Uyama Y, Ikada Y. Polymer surface with graft chains. Prog Polym Sci 2003;28:209–59. 10.1016/s0079-6700(02)00032-1

[112] Kim DJ, Kang SM, Kong B, Kim WJ, Paik HJ, Choi H, Choi IS. Formation of thermoresponsive gold nanoparticle/PNIPAAm hybrids by surface-initiated, atom transfer radical polymerization in aqueous media. Macromol Chem Phys 2005;206:1941–6. 10.1002/macp.200500268

[113] Raula J, Shan J, Nuopponen M, Niskanen A, Jiang H, Kauppinen EI, Tenhu H. Synthesis of gold nanoparticles grafted with a thermoresponsive polymer by surface-induced reversible-addition-fragmentation chain-transfer polymerization. Langmuir 2003;19:3499–504. 10.1021/la026872r

[114] Mandal TK, Fleming MS, Walt DR. Preparation of polymer coated gold nanoparticles by surface-confined living radical polymerization at ambient temperature. Nano Lett 2002;2:3–7. 10.1021/nl015582c

[115] Yoon KR, Ramaraj B, Lee SM, Kim D-P. Surface initiated-atom transfer radical polymerization of a sugar methacrylate on gold nanoparticles. Surf Interface Anal 2008;40:1139–43. 10.1002/sia.2847

[116] Li D, He Q, Cui Y, Li J. Fabrication of pH-responsive nanocomposites of gold nanoparticles/poly(4-vinylpyridine). Chem Mater 2007;19:412–7. 10.1021/cm062290+

[117] Suzuki D, Kawaguchi H. Modification of gold nanoparticle composite nanostructures using thermosensitive core-shell particles as a template. Langmuir 2005;21:8175–9. 10.1021/la0504356

[118] Corbierre MK, Cameron NS, Sutton M, Laaziri K, Lennox RB. Gold nanoparticle/polymer nanocomposites: Dispersion of nanoparticles as a function of capping agent molecular weight and grafting density. Langmuir 2005;21:6063–72. 10.1021/la047193e

[119] Wang L, Kariuki NN, Schadt M, Mott D, Luo J, Zhong C-J, Shi X, Zhang C, Hao W, Lu S, Kim N, Wang J-Q. Sensing arrays constructed from nanoparticle thin films and interdigitated microelectrodes. Sensors 2006;6:667–79. 10.3390/s6060667

[120] Salvati R, Longo A, Carotenuto G, De Nicola S, Pepe GP, Nicolais L, Barone A. UV-vis spectroscopy for on-line monitoring of Au nanoparticles size during growth. Appl Surf Sci 2005;248:28–31. 10.1016/j.apsusc.2005.03.075

[121] Saha K, Agasti SS, Kim C, Li X, Rotello VM. Gold nanoparticles in chemical and biological sensing. Chem Rev 2012;112:2739–79. 10.1021/cr2001178

[122] Kang YJ, Taton TA. Core/shell gold nanoparticles by self-assembly and crosslinking of micellar, block-copolymer shells. Angew Chem-Int Edit 2005;44:409–12. 10.1002/anie.200461119

[123] Chui YH, Grochola G, Snook IK, Russo SP. Molecular dynamics investigation of the structural and thermodynamic properties of gold nanoclusters of different morphologies. Phys Rev B 2007;75:1–8. 10.1103/PhysRevB.75.033404

[124] Mayoral A, Barron H, Estrada-Salas R, Vazquez-Duran A, Jose-Yacaman M. Nanoparticle stability from the nano to the meso interval. Nanoscale 2010;2:335–42. 10.1039/b9nr00287a

[125] Reznickova A, Kolska Z, Zaruba K, Svorcik V. Grafting of gold nanoparticles on polyethyleneterephthalate using dithiol interlayer. Mater Chem Phys 2014;145:484–90. 10.1016/j.matchemphys.2014.03.001

[126] Reznickova A, Novotna Z, Kolska Z, Svorcik V. Immobilization of silver nanoparticles on polyethylene terephthalate. Nanoscale Res Lett 2014;9:1–6. 10.1186/1556-276x-9-305

[127] Rezanka P, Rezankova H, Matejka P, Kral V. The chemometric analysis of UV-visible spectra as a new approach to the study of the NaCl influence on aggregation of cysteine-capped gold nanoparticles. Colloids Surfaces A Physicochem Eng Aspects 2010;364:94–8. 10.1016/j.colsurfa.2010.05.001

[128] Luis Elechiguerra J, Reyes-Gasga J, Jose Yacaman M. The role of twinning in shape evolution of anisotropic noble metal nanostructures. J Mater Chem 2006;16:3906–19. 10.1039/b607128g

[129] Yin J, Yang Y, Hu Z, Deng B. Attachment of silver nanoparticles (AgNPs) onto thin-film composite (TFC) membranes through covalent bonding to reduce membrane biofouling. J Membr Sci 2013;441:73–82. 10.1016/j.memsci.2013.03.060

[130] Chu PK, Chen JY, Wang LP, Huang N. Plasma-surface modification of biomaterials. Mat Sci Eng R 2002;36:143–206. 10.1016/s0927-796x(02)00004-9

[131] Gam-Derouich S, Mahouche-Chergui S, Truong S, Ben Hassen-Chehimi D, Chehimi MM. Design of molecularly imprinted polymer grafts with embedded gold nanoparticles through the interfacial chemistry of aryl diazonium salts. Polymer 2011;52:4463–70. 10.1016/j.polymer.2011.08.007

[132] Guerrouache M, Mahouche-Chergui S, Chehimi MM, Carbonnier B. Site-specific immobilisation of gold nanoparticles on a porous monolith surface by using a thiol-yne click photopatterning approach. Chem Commun 2012;48:7486–8. 10.1039/c2cc33134a

[133] Carey FA, Sundberg RJ. Advanced Organic Chemistry. 4 ed. New York: Plenum Press; 1993. 286 p.

[134] Reznickova A, Kolska Z, Hnatowicz V, Stopka P, Svorcik V. Comparison of glow argon plasma-induced surface changes of thermoplastic polymers. Nucl Instrum Methods Phys Res, Sect B 2011;269:83–8. 10.1016/j.nimb.2010.11.018